

Modeling early stages of endoderm development in epiblast stem cell aggregates with supply of extracellular matrices

Sachiko Inamori¹ | Mai Fujii¹ | Sayaka Satake¹ | Hideaki Iida¹ | Machiko Teramoto¹ | Tomoyuki Sumi² | Chikara Meno² | Yasuo Ishii^{1,3} | Hisato Kondoh¹ 

¹Faculty of Life Sciences and Institutes for Protein Dynamics and Comprehensive Research, Kyoto Sangyo University, Kyoto, Japan

²Department of Developmental Biology, Graduate School of Medical Sciences, Kyushu University, Fukuoka, Japan

³Department of Biology, School of Medicine, Tokyo Women's Medical University, Tokyo, Japan

Correspondence

Hisato Kondoh, Faculty of Life Sciences and Institutes for Protein Dynamics and Comprehensive Research, Kyoto Sangyo University, Kita-ku, Kyoto 603-8555, Japan. Email: kondohh@cc.kyoto-su.ac.jp

Funding information

MEXT; Kyoto Sangyo University; MEXT Grants-in-Aid for Scientific Research, Grant/Award Number: JP17H03688 and JP19K16184

[Correction added on 19 May 2020, after first online publication: the grant number has been amended in the Funding information and Acknowledgment section.]

Abstract

Endoderm precursors expressing *FoxA2* and *Sox17* develop from the epiblast through the gastrulation process. In this study, we developed an experimental system to model the endoderm-generating gastrulation process using epiblast stem cells (EpiSCs). To this end, we established an EpiSC line i22, in which enhanced green fluorescent protein is coexpressed with *Foxa2*. Culturing i22 EpiSCs as aggregates for a few days was sufficient to initiate *Foxa2* expression, and further culturing of the aggregates in Matrigel promoted the sequential activation of transcription factor genes involved in endoderm precursor development, e.g., *Eomes*, *Gsc*, and *Sox17*. In aggregation culture of i22 cells for 3 days, all cells expressed POU5F1, SOX2, and E-cadherin, a signature of the epiblast, whereas expression of GATA4 and SOX17 was also activated moderately in dispersed cells, suggesting priming of these cells to endodermal development. Embedding the aggregates in Matrigel for further 3 days elicited migration of the cells into the lumen of laminin-rich matrices covering the aggregates, in which FOXA2 and SOX17 were expressed at a high level with the concomitant loss of E-cadherin, indicating the migratory phase of endodermal precursors. Prolonged culturing of the aggregates generated three segregating cell populations found in post-gastrulation stage embryos: (1) definitive endoderm co-expressing high SOX17, GATA4, and E-cadherin, (2) mesodermal cells expressing a low level of GATA4 and lacking E-cadherin, and (3) primed epiblast cells expressing POU5F1, SOX2 without E-cadherin. Thus, aggregation of EpiSCs followed by embedding of aggregates in the laminin-rich matrix models the gastrulation-dependent endoderm precursor development.

KEYWORDS

endoderm, epiblast stem cells, extracellular matrix, FOXA2, gastrulation

Inamori and Fujii contributed equally to this study.

This is an open access article under the terms of the Creative Commons Attribution-NonCommercial License, which permits use, distribution and reproduction in any medium, provided the original work is properly cited and is not used for commercial purposes.

© 2020 The Authors. *Development, Growth & Differentiation* published by John Wiley & Sons Australia, Ltd on behalf of Japanese Society of Developmental Biologists

1 | INTRODUCTION

In vertebrate embryos, establishment of the epiblast, the precursor for all somatic lineages, is followed by the gastrulation process that derives and spatially arranges various early somatic tissues. The gastrulation process occurs in the node-proximal region and also along the posteriorly extending primitive streak. Endoderm, the focus of this study, develops primarily via the node-proximal gastrulation process, and characterized by the co-expression of transcription factors (TFs) FOXA2 and SOX17 (Burtscher & Lickert, 2009; Nowotschin, Hadjantonakis, & Campbell, 2019; Viotti, Nowotschin, & Hadjantonakis, 2014). In this study, we established an experimental system to investigate molecular and cellular mechanisms underlying the derivation of endoderm precursors and endoderm tissues, modeled in epiblast stem cells (EpiSCs). This approach circumvents the hurdle in reaching and manipulating epiblast cells located deep inside of egg cylinder stage mouse embryos.

Mouse EpiSCs, representing to a large extent the egg cylinder stage epiblast (Brons et al., 2007; Tesar et al., 2007), are useful in the investigation of epiblast-derived developmental processes (e.g., Iwafuchi-Doi et al., 2012; Teo et al., 2011). Although culture protocols to obtain endoderm precursors from EpiSCs under spreading culture conditions are available, EpiSCs are placed under artificial conditions, with daily changes in exogenous signal inputs including high Activin, BMP and PI-3 kinase blocker LY294002 (Teo et al., 2011). We postulated that a more cell autonomy-dependent experimental system using cell culture will be required to gain insight into the cell regulatory processes to derive endoderm that occurs in embryos. In normal embryos, endoderm precursors develop, starting from the node-proximal region of the epiblast that expresses TF FOXA2 (Burtscher & Lickert, 2009). A knockin mouse line expressing enhanced green fluorescent protein (EGFP) with the same specificity as FOXA2 is available (Imuta, Kiyonari, Jang, Behringer, & Sasaki, 2013), in which the EGFP coding sequence was inserted via the 2A peptide sequence immediately 3' of the FOXA2-coding sequence. EpiSC lines carrying this *Foxa2-Egfp* gene will be useful in investigating early stages of endoderm development. An advantage of using EpiSCs over embryonic stem cells (ESCs) in investigating definitive endoderm is that EpiSCs produce only embryonic (definitive) endoderm, whereas ESC-originated lineages are complex, deriving extraembryonic (primitive) endoderm tissues expressing *Sox7* and *Sox17*, and epiblast first, from the latter of which definitive embryonic endoderm expressing only *Sox17* develops (Kinoshita, Shimosato, Yamane, & Niwa, 2015).

Recent investigations on EpiSC derivation indicated that attenuating Wnt signals facilitates the establishment of stable EpiSC lines (Sugimoto et al., 2015; Sumi, Oki, Kitajima, & Meno, 2013). As Wnt signal attenuation may predispose EpiSCs to developmental processes in the anterior domain of embryos (Matsuda & Kondoh, 2014), such EpiSC lines may be particularly useful in the study of node-proximal gastrulation. We thus established an EpiSC line i22 from *Foxa2-Egfp* knockin mouse embryos using a moderate level of Wnt signal inhibitor XAV939.

We investigated the culture conditions for i22 EpiSCs to express *Foxa2*-dependent EGFP (*Foxa2*-EGFP) and endoderm-associated TF

genes. We found that aggregation of i22 cells in the ordinary EpiSC maintenance culture medium in nonadherent culture dishes was sufficient for activating the *Foxa2*-EGFP expression, suggesting priming of the gastrulation process. Then, suspending the aggregates in Matrigel, which allows cells on the aggregate surface to interact with the laminin-rich extracellular matrix, elicited the sequential activation of endoderm-characteristic TF genes, *Eomesodermin* (*Eomes*), *Gooseoid* (*Gsc*), and *Sox17* (Arnold, Hofmann, Bikoff, & Robertson, 2008; Kanai-Azuma et al., 2002; Teo et al., 2011). The same condition also activated cardiac lineage TF genes, *Mesp1*, *Gata6*, and *Gata4*, indicating that provision of the extracellular matrix promoted endodermal and cardiac precursor development. At the cellular level, the SOX17-expressing cells developed as a subpopulation of GATA4-expressing cells, suggesting the possibility of sharing of precursors between the endodermal and cardiac lineages. Thus, using a genetically labeled EpiSC line, a model system has been established to investigate the node-proximal gastrulation process to derive endoderm tissues.

2 | MATERIALS AND METHODS

2.1 | Handling of EpiSCs

i22 EpiSC line was established from a homozygous *Foxa2-Egfp* knockin mouse embryo of B6/DBA2 hybrid background, using the procedure previously described by Sumi et al. (2013), with the modification of placing cells in a feeder-free culture condition from passage 3 using the medium described by Iwafuchi-Doi et al. (2012) with addition of 2 μ M XAV939. To prepare i22 cell aggregates, the dish-attached i22 cells were dissociated using Accutase (Nacalai) and added on a nonadherent dish at a concentration of 4×10^5 cells/2 ml culture medium. Starting on day 2 when cell aggregates were formed, aggregates were diluted serially to minimize fusion of aggregates. To embed the aggregates in growth factor-depleted Matrigel (Corning), several aggregates suspended in 60 μ l culture medium were mixed with 100 μ l chilled Matrigel liquid and poured into a 1 cm diameter well of a glass-bottomed dish (Matsunami). After solidification of Matrigel at 37°C for 10 min, the well was overlaid with 2 ml of the culture medium. To obtain dissociated cells to apply to FACS Melody for cell fractionation, the aggregates in Matrigel were treated with Dispase II (Wako) at 10 μ g/ml at 37°C to remove adhering Matrigel, and dissociated into single cells using Accutase with 0.05% Trypsin and 1 mM EDTA. To produce teratoma, a Balb/c nude mouse was injected intraperitoneally with 10^6 i22 cells, and a teratoma mass was surgically isolated after 2 months.

2.2 | Histological analyses

To obtain hematoxylin-eosin-stained sections, teratoma masses were fixed with Bouin's fixative, and embedded in paraffin. For immunostaining of cells in adhering cultures or in aggregates, cells

were fixed with 4% paraformaldehyde. The aggregates were further processed for cryosectioning. The cells on dishes or in sections were stained using the combinations of antibodies shown in Table 1. Immunostaining of ICR mouse embryos was performed according to Burtscher and Lickert (2009). Photo-images were captured using Axioplan 2 (Zeiss), DMI 6000B inverted microscope (Leica), or FV3000 laser microscope (Olympus). Linear level adjustment of color channels and pseudo color operation were performed using FIJI (Schindelin et al., 2012).

2.3 | RT-qPCR analysis

RNAs were extracted using TRIzol™ Plus RNA Purification Kit (Thermo Fisher), reverse-transcribed using SuperScript III (Thermo Fisher), and treated with RNaseH (Takara). qPCRs were performed using primers listed in Table 2 and TB Green Premix ExTaq II (Takara) with PCR cycles of 5 s at 95°C and 30 s at 60°C in QuantoStudio3 Real-time PCR system (Applied Biosystems). The data were expressed as the relative molecular abundance compared to *Gapdh* mRNA.

3 | RESULTS

3.1 | Establishment of an EpiSC line carrying the *Foxa2-Egfp* knockin gene

We crossed the *Foxa2-Egfp* knockin mouse of ICR background produced by Imuta et al. (2013) with mice of C57BL/6/DBA2 hybrid background for several generations, and *Foxa2-Egfp* homozygous mice were maintained. EpiSC lines were produced from the epiblast of E6.5 stage embryos according to the procedure described by Sumi et al. (2013). The culture medium containing 10 ng/ml activin, 10 μM XAV939 (a tankyrase inhibitor which suppresses Wnt/β-catenin signaling) and 20% Knockout serum replacement (Thermo Fisher) and using feeder cells up to initial two passages,

but from the next passage, culture medium was switched to a feeder-free culture condition containing 20 ng/ml activin, 10 ng/ml FGF2 (Iwafuchi-Doi et al., 2012) with supplement of 2 μM XAV939. One of the cell lines, i22, was used in this study after 20 passages (Figure 1a). The i22 cells showed typical morphology of EpiSCs (Brons et al., 2007; Iwafuchi-Doi et al., 2012; Tesar et al., 2007), expressed nuclear POU5F1 and SOX2, as examined by immunostaining (Figure 1b), a basic feature of EpiSCs. Moreover, injection of i22 cells into the peritoneal cavity of immunodeficient mice resulted in the development of well-differentiated teratoma tissues (Figure 1c). From these observations, we concluded that i22 is a pluripotent EpiSC line.

3.2 | Development of *Foxa2*-EGFP-expressing cells in i22 cell aggregates

We considered the possibility that floating cell aggregates of EpiSCs formed in nonadherent culture dishes may elicit somatic development of EpiSCs, considering the precedents of ESC-derived embryoid bodies and various tissue organoids that develop under analogous conditions (McCauley & Wells, 2017; Simunovic & Brivanlou, 2017, for review), and anticipated that *Foxa2*-EGFP expression would occur if the endodermal developmental pathway is activated. We thus prepared aggregates of i22 cells in a nonadherent culture dish using the same culture medium as that used in EpiSC maintenance. A low level (2 μM) of XAV939 was continuously supplied, because in adherence cultures, removal of XAV939 destabilized the i22 cells, and also because suppression of Wnt signaling may promote the gastrulation process around the node and anterior primitive streak.

The aggregation culture of i22 cells for a few days was sufficient to activate *Foxa2*-EGFP expression (Figure 2a (D2 and D3)), which was not observed in i22 cells in dish-adherent cultures (Figure 2a (D1)). This observation suggested that formation of floating cell aggregates is sufficient to cause the *Foxa2*-expressing, gastrulation-ready cell states. *Foxa2*-EGFP expression level reached its peak at day 3 (D3) in floating aggregation culture.

TABLE 1 Antibodies used for immunofluorescence staining

Antigen	Primary antibodies			Secondary antibodies (Donkey, Abcam)			
	Animal	Provider	Product	Dilution	Alexa #	Product	Dilution
E-cad	Mouse	Abcam	ab76055	1/250	647	ab150107	1/800
FOXA2	Mouse	Abcam	ab60721	1/50	647	ab150107	1/800
GATA4 ^a	Rabbit	Abcam	ab61767	1/40	568	ab175692	1/800
GFP	Rabbit	MBL	598	1/1,000	488	ab150061	1/800
Laminin ^b	Rabbit	Abcam	ab11575	1/500	568	ab175692	1/800
POU5F1	Goat	SANTA CRUZ	sc-11661	1/400	488	ab150133	1/800
SOX2	Rabbit	MBL	PM056	1/400	568	ab175692	1/800
SOX17	Goat	Neuromics	GT15094	1/500	488	ab150133	1/800

^aThese antibodies showed a low cross reactivity against a component of Matrigel.

^bThe antigen was Matrigel-derived laminin, comprising α1, β1, and γ1 chains.

Target genes	Primer sequences (F, forward, R, reverse)	PCR product length (bp)	References
<i>Gapdh</i>	F: CATGGCCTTCCGTGTTCTCA R: GCGGCACGTCAATCCA	55	Iwafuchi-Doi et al. (2012)
<i>Pou5f1</i>	F: TTCCTCTGTTCCCGTCACT R: TGGTGCCTCAGTTTGAATGC	57	Iwafuchi-Doi et al. (2012)
<i>Sox2</i>	F: CCATGGGCTCTGTGGTCAAG R: CCCTGGAGTGGGAGGAAGAG	72	Iwafuchi-Doi et al. (2012)
<i>Nanog</i>	F: AGGCCTGGACCGCTCAGT R: AGTTATGGAGCGGAGCAGCAT	60	Iwafuchi-Doi et al. (2012)
<i>Brachyury</i>	F: TTGAACCTTCTCCATGTGCTGA R: TCCCAAGAGCCTGCCACTTT	82	Iwafuchi-Doi et al. (2012)
<i>Eomes</i>	F: GCCTTCCACCTTTGATGTATCC R: AAAGCTTTGGCGCCTTCTCT	61	Iwafuchi-Doi et al. (2012)
<i>Gsc</i>	F: CCAGCAGTGCTCCTGCGTCC R: CGACAGCGTCCCACGTTCA	620	van den Aamele et al. (2012)
<i>Sox17</i>	F: ATAAGCCCGAGATGGGTCTTC R: CCGTGGCTGTCTGAGAGGTT	67	Iwafuchi-Doi et al. (2012)
<i>Mesp1</i>	F: TGTACGCAGAAACAGCATCC R: TTGTCCCCTCCACTCTTCAG	144	van den Aamele et al. (2012)
<i>Gata6</i>	F: GACTGTCTGTGCCAACTGTCA R: TGGAGTTTCATATAGAGCCCGC	103	This study
<i>Gata4</i>	F: GCCCAAGAACCTGAATAAAT R: CGGACACAGTACTGAATGTCT	209	This study
<i>Sox7</i>	F: AGATGCTGGAAAGTCATGG R: GCTTGCCTGTTTCTTCTG	141	Kinoshita et al. (2015)
<i>Laminin α1</i>	F: TGGAGACGGTGACAGTGACCT R: CAGCCACTGCCAAGTCTATAGCA	321	Futaki et al. (2019)
<i>Laminin α4</i>	F: AGAATCTCTGTGATGGCAGATGG R: GCAGCTTTACTGAAGCTCACAGG	256	Futaki et al. (2019)
<i>Laminin α5</i>	F: TGGCTCCTACCTGGATGGCAG R: CTCCACACGCACCAACACACG	307	Futaki et al. (2019)

TABLE 2 Primers used in RT-qPCR analysis

Immunostaining of cryosections of D3 i22 cell aggregates demonstrated that variable levels of *Foxa2*-EGFP were expressed in the majority of cells (Figure 2b). SOX17 was sporadically expressed in cells with high *Foxa2*-EGFP expression (Figure 2b(i), arrowheads), whereas GATA4 was more widely expressed at a modest level without much correlation with the *Foxa2*-EGFP expression level (Figure 2b(ii)). This observation indicated that the developmental pathway leading to endoderm development had been primed, at least, in the D3 aggregates. However, in the extended culture of free-floating (FF) aggregates, the EGFP fluorescence diminished (Figure 2c).

Considering the *in vivo* situation, gastrulating epiblast cells are underlain by the laminin-rich basement membrane, and the cells undergo gastrulation by disrupting the basement membrane to migrate into the endodermal (external) layer (Burtscher & Lickert, 2009). We, therefore, reasoned that to mimic gastrulation processes, interaction of EpiSCs with laminin-rich basement membrane analogs may be required. Thus, we embedded the preformed D3 EpiSC aggregates in the growth factor-depleted Matrigel, and compared the aggregate development with that under FF condition. Whereas Matrigel-embedded cell aggregates (Mt) developed further as spherical structures, and maintained *Foxa2*-EGFP expression (Figure 2d), the FF

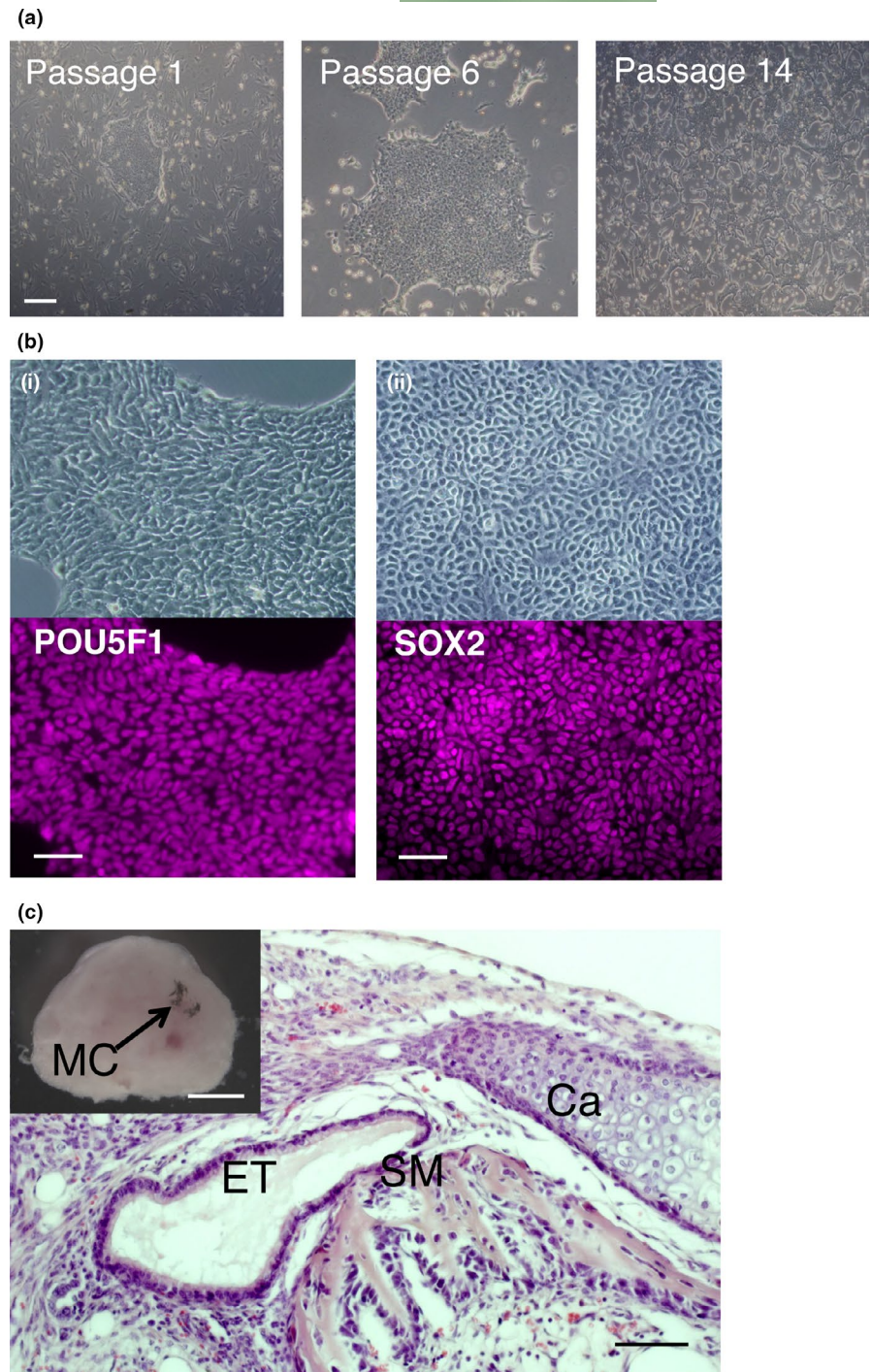
aggregates developed with irregular shapes in addition to the gradual loss of *Foxa2*-EGFP expression, as indicated above (Figure 2c).

3.3 | Changes in TF gene expression profiles of i22-derived cells in cell aggregates and following Matrigel embedding

To characterize the cellular and molecular events occurring in i22 cell aggregates, we investigated the expression profiles of lineage-characteristic TF genes. Cell aggregates were harvested at intervals for RNA isolation, the aggregates being split into those with (Mt) or without Matrigel embedding (FF) after 3 days. Then changes in gene expression levels were assessed by using RT-qPCR, as summarized in Figure 3.

The representative TF genes expressed in EpiSCs, i.e., *Pou5f1*, *Sox2*, and *Nanog* (Brons et al., 2007; Iwafuchi-Doi et al., 2012; Tesar et al., 2007), remained to be expressed in the FF aggregates even at D6, indicating that a substantial fraction of cells in the i22 aggregates remained as epiblast-like state (Figure 3a). In contrast to the case of *Pou5f1* and *Nanog*, where expression levels were lower in D6-Mt

FIGURE 1 Outline of the procedure to establish the i22 line, and its verification as an EpiSC line. (a) Changes in cell cluster appearance before attaining the morphologically stable state after passage 10. Phase-contrasted images of live cells are shown. Bar, 200 μm . (b) Phase-contrasted images of a region of i22 cell clusters (top) and their immunofluorescence images for (i) POU5F1 and (ii) SOX2 (bottom). Bar, 100 μm . (c) A teratoma mass that developed from i22 EpiSCs intraperitoneally injected in an immunodeficient mouse (inset) and its histological section stained by hematoxylin and eosin. Abbreviations: MC, melanocytes; ET, epithelial tube; Ca, cartilage; SM, skeletal muscle. Bars, 200 μm for main panel and 2 mm for inset

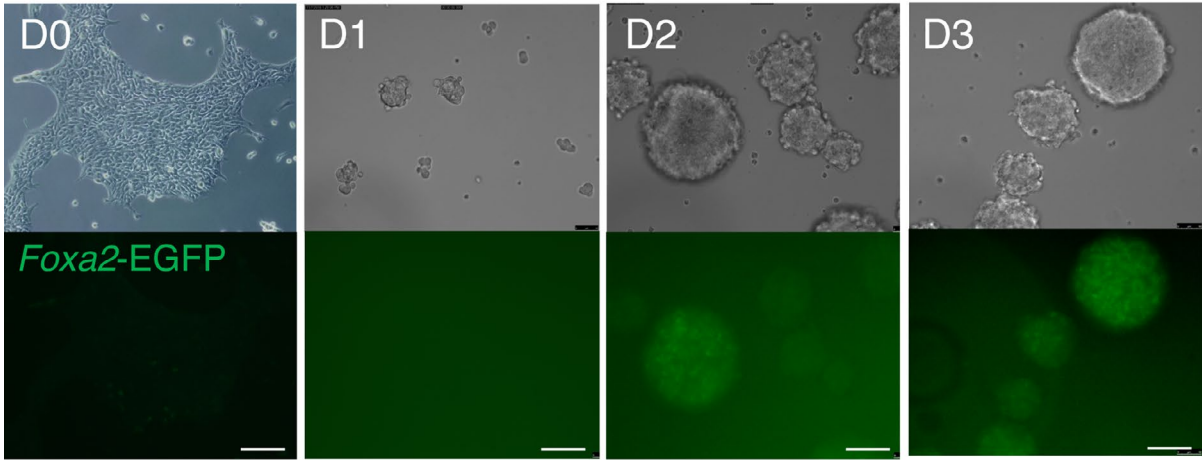


than in D6-FF, the *Sox2* level in D6-Mt was higher than that in D6-FF. Considering the immunohistology data shown below (Figures 5 and 6), these data suggest that the *Sox2* level in a cell was augmented in D6-Mt cells. The discordance of the *Sox2* and *Pou5f1* expression levels presumably reflects the fact that SOX2 and POU5F1 function almost independently in EpiSCs (Matsuda et al., 2017).

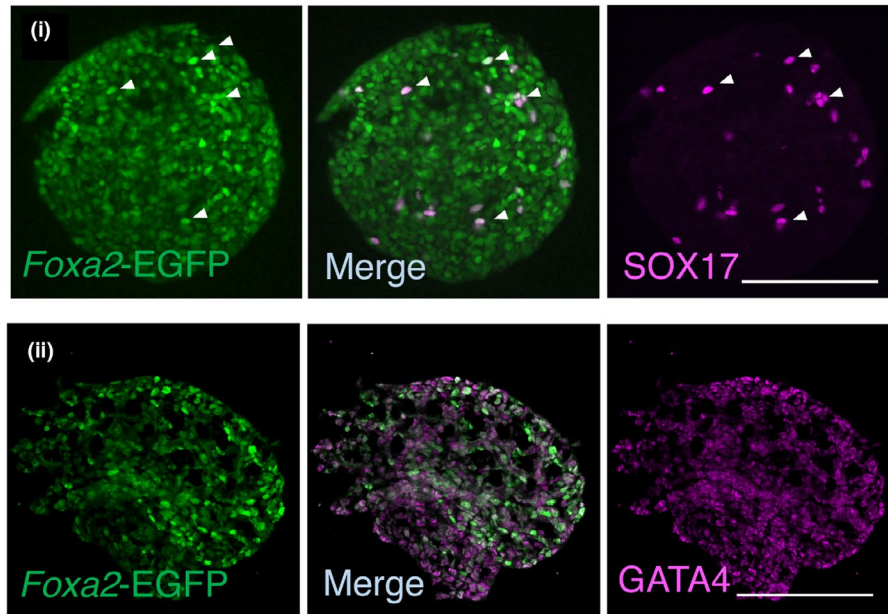
The *Brachyury* (*Bra/T*) gene involved in the prechordal plate/notochord development and in the primitive streak-mediated developmental process was sharply activated in 2 days of aggregation, but was then quickly downregulated in further cultivation of aggregates, regardless of Matrigel embedding (Figure 3b).

Among the TF genes involved in the development of endodermal lineage, the *Eomesodermin* (*Eomes*) gene, which is activated in the initial step of endoderm development (Arnold et al., 2008; Teo et al., 2011), was quickly activated and then downregulated in the aggregates following the time course similar to *Bra* expression (Figure 3b). This *Eomes* activation was followed by the sequential activation of *Gooseoid* (*Gsc*) and *Sox17* (the hallmark of definitive endoderm development), which recapitulates the normal time course of endoderm development in vivo (Kanai-Azuma et al., 2002; Tada et al., 2005; Teo et al., 2011). Although *Sox17* expression was not maintained in FF aggregates, those developed

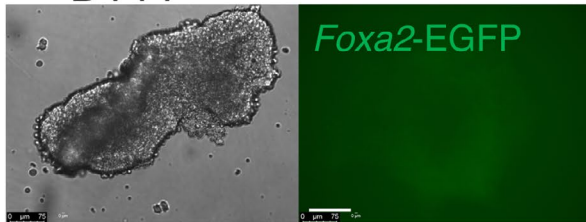
(a)



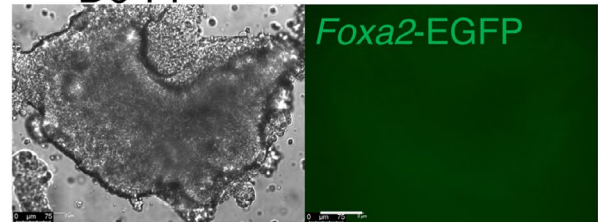
(b) D3



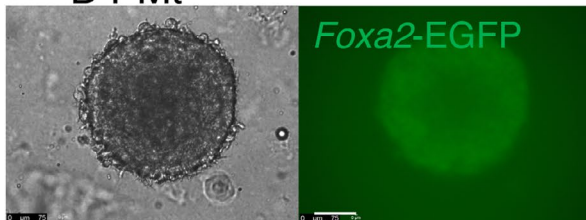
(c) D4-FF



D6-FF



(d) D4-Mt



D6-Mt

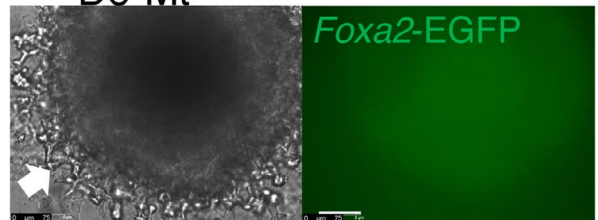


FIGURE 2 Activation of *Foxa2*-EGFP in i22 EpiSC aggregates, and the effect of embedding the aggregates in Matrigel. (a) Emergence of *Foxa2*-EGFP expressing cells. "D" indicates the days in aggregates, whereas "D0" indicates the i22 cells on a culture dish before harvesting. Top and bottom, photo-transmission images and EGFP fluorescence images, respectively. (b) Cross sections of D3 aggregates immunostained for GFP to detect *Foxa2*-EGFP expression (green), and also for (i) SOX17 and (ii) GATA4 (magenta). Merged fluorescent images (ii) are also shown. Note that high SOX17 expression (arrowheads) occurred in cells expressing *Foxa2*-EGFP at a high level. (c) and (d) Morphological changes of aggregates (left) and *Foxa2*-EGFP fluorescence (right) in the free-floating (FF) (c) or aggregates embedded in Matrigel (Mt) (d). D4 and D6 data are of the same aggregate. Note that FF aggregates lost their spherical shape and also EGFP fluorescence, whereas the Mt aggregates maintained *Foxa2*-EGFP fluorescence, increased in external diameter, and were covered by cells migrating into the Matrigel space (white arrow at D6). Bars, 100 μ m

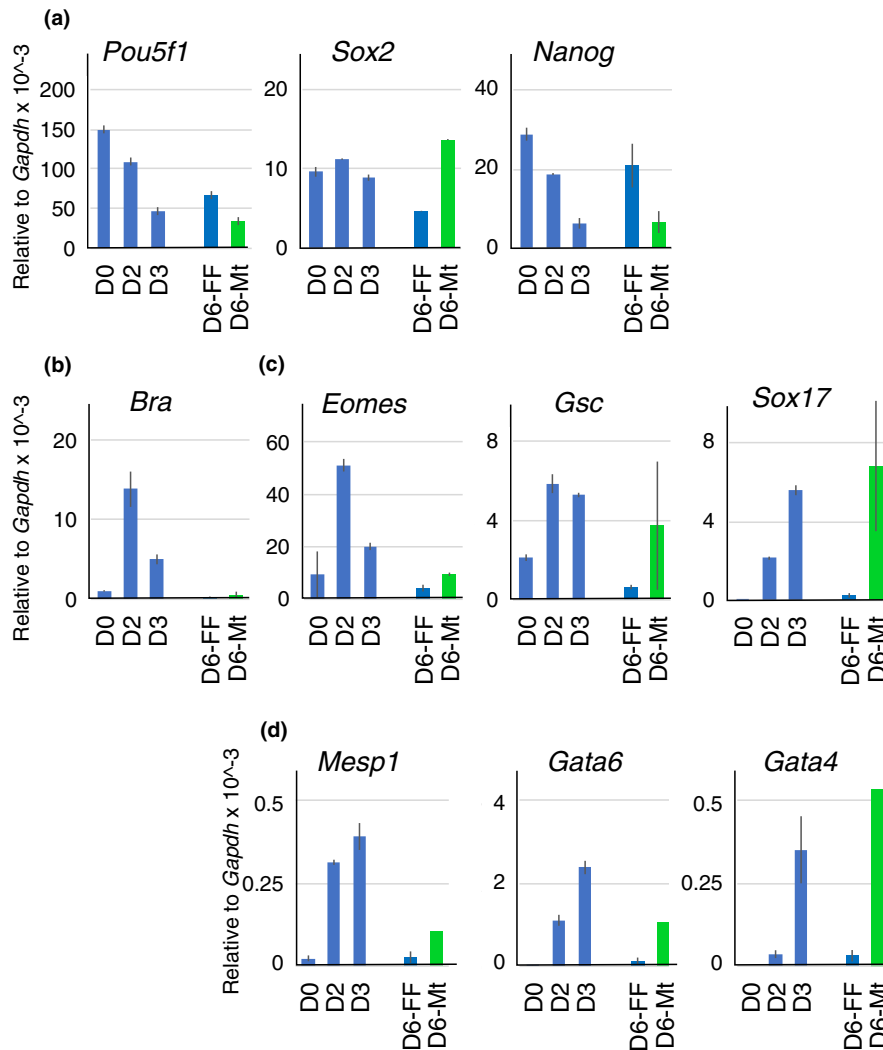


FIGURE 3 Time course changes in transcript levels of TF genes characteristics of epiblast and/or specific somatic lineages in i22 cell aggregates and in Matrigel. Two independent i22 aggregate cultures were prepared, and a group of aggregates in each culture was sampled for RT-qPCR analysis. At day 3 (D3) of culture starting from adherent i22 culture (D0), each culture was split into two groups, the one which was kept as free-floating (FF) culture condition, and another which was embedded in Matrigel (Mt). The transcript levels are shown relative to *Gapdh* level, and error bars indicate the data range of two samples. (a) TF genes characteristic of epiblast state: *Pou5f1*, *Sox2*, and *Nanog*. (b) *Brachyury* (*Bra/T*), expressed in the prechordal plate/notochord and primitive streak. (c) TFs expressed in the endodermal precursors: *Eomesodermin* (*Eomes*), *Gooseoid* (*Gsc*), and *Sox17*. The large data range for the *Gsc* D6-Mt samples presumably reflects an asynchrony of molecular events between different aggregate samples, exemplified by the differences in developmental stages of aggregates shown in Figures 4 and 5, derived from different batches of D6-Mt cultures. Such differences may have been caused by the heterogeneity of initial aggregate sizes, as shown in Figure 2a. (d) TFs expressed in the cardiac lineages: (i) *Mesp1*, (ii) *Gata6*, and (iii) *Gata4*. The D6-Mt data are derived from a single sample, but the reproducibility of data was confirmed by comparison with FACS-sorted samples shown in Figure 8

in Matrigel maintained *Sox17* expression (Figure 3c), suggesting that endoderm development proceeded in the supply of basement membrane components.

In cardiac lineage development, TF genes *Mesp1*, *Gata6* and *Gata4* are activated in sequence (Charron & Nemer, 1999; Kuo et al., 1997; Molkenin, Lin, Duncan, & Olson, 1997; Saga et al., 1999;

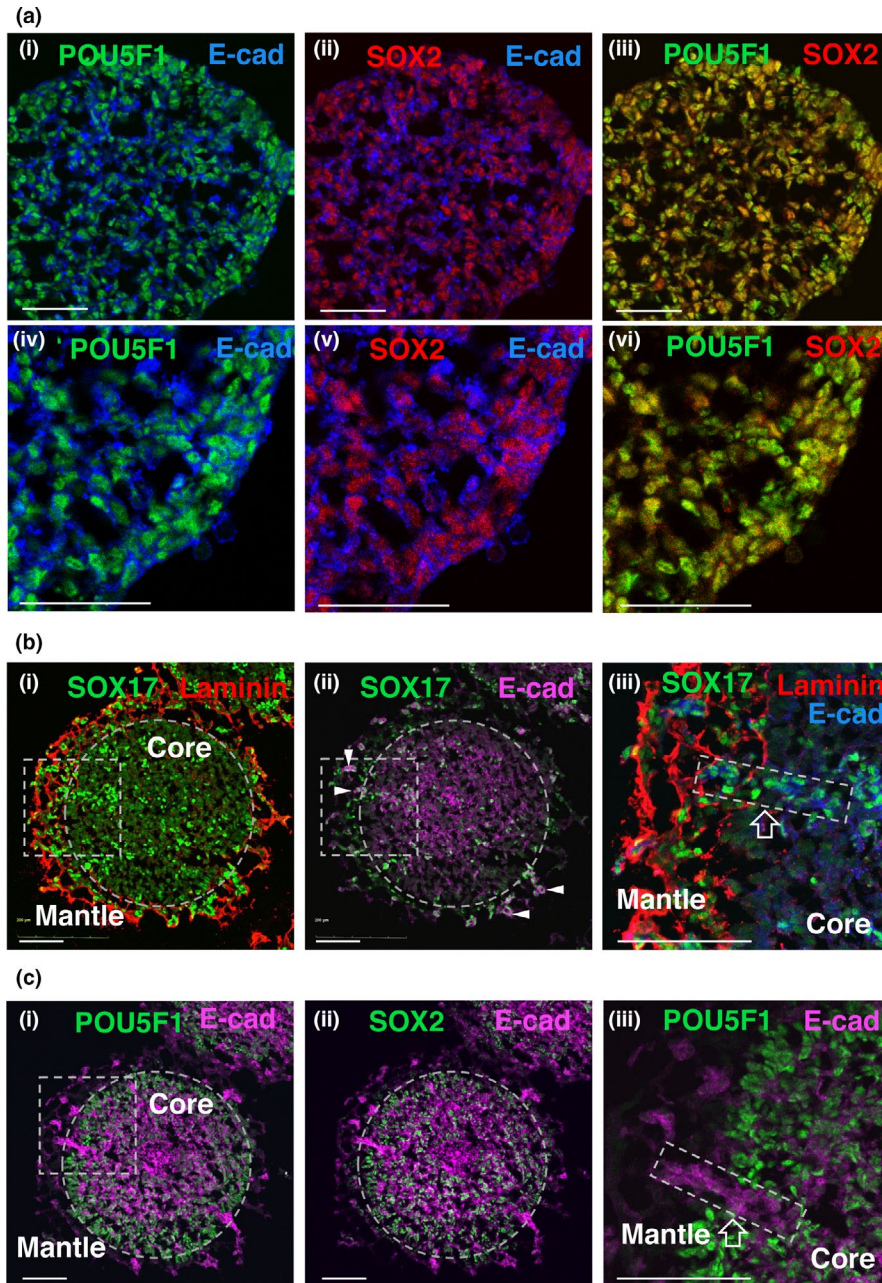


FIGURE 4 Embedding of EpiSC aggregates in Matrigel triggers the exit of cells from the epiblast state into endoderm and related lineages. (a) The same section of a D3 aggregate immunostained for POU5F1, SOX2, and E-cadherin, shown in pairwise combination of immunofluorescence: (i) POU5F1 and E-cadherin (E-cad), (ii) SOX2 and E-cad, and (iii) POU5F1 and SOX2. (iv) to (v) show high power views of their right-bottom sectors. (b) The same section of a D6-Mt aggregate immunostained for SOX17, laminin, and E-cadherin. (i) Superimposed immunofluorescence images of SOX17 and laminin. The rough boundary of laminin-free core zone (Core) is encircled by a broken line. (ii) The same section shown for SOX17 and E-cad expression, indicating that the majority of SOX17-expressing cells were free from or low in E-cadherin expression, whereas some SOX17-expressing cell clusters expressed a high level of E-cadherin (arrowheads). (iii) A high power view of the area indicated by a rectangle in (i) and (ii). The broken rectangle with an arrow indicates a stream-like SOX17-expressing cell cluster with strong E-cad expression, penetrating the boundary between the core and mantle zones. (c) An adjacent section of the same aggregate shown in (b), stained for POU5F1, SOX2, and E-cadherin. (i) and (iii) Comparison of POU5F1 and E-cad expression, and (ii) comparison of SOX2 and E-cad expression, showing that most of the cells in the core zone coexpressed POU5F1 and SOX2. The broken rectangle with an arrow indicates the same as (b)(iii). Bars, 50 μm for (a) and 100 μm for (b) and (c)

Zhao et al., 2008), although *Gata6* and *Gata4* are also expressed and play essential regulatory roles in endoderm development (Bossard & Zaret, 1998; Fisher, Pulakanti, Rao, & Duncan, 2017; Molkentin, 2000; Simon et al., 2018; Teo et al., 2011). It was interesting to note that in i22 aggregates, these TF genes, starting from *Mesp1*, were activated in this order, and a high *Gata4* expression was maintained only in Matrigel-embedded aggregates (Figure 3d), similar to the case of endodermal *Sox17* expression (Figure 3c). *Mesp1* expression was already high at D2, but its level was maintained to D3, in contrast to the sharp decline of *Eom*s expression at D3. This presumably reflects the fact that *Mesp1* activation depends on the *Eom*s expression (van den Ameel et al., 2012), causing some delay in the peaking of *Mesp1* expression compare to *Eom*s.

The analysis of TF genes expression and its time course overall suggested that EpiSC aggregate formation is sufficient to prime cells for

various somatic lineage developments. However, these primed states were not maintained in simple FF aggregates. Nevertheless, embedding the aggregates in Matrigel provided extracellular matrix to mimic the epiblast-underlying basement membrane, and the developmental process for endodermal and cardiac development was actuated.

3.4 | Exit of the epiblast into the endodermal lineage via provoking migratory cell state in Matrigel-embedded aggregates

To determine the cell states and tissue organization in the i22 aggregates at different time points of culturing aggregates in Matrigel, we performed immunohistological analysis for the expression of TFs and epithelium-associated E-cadherin.

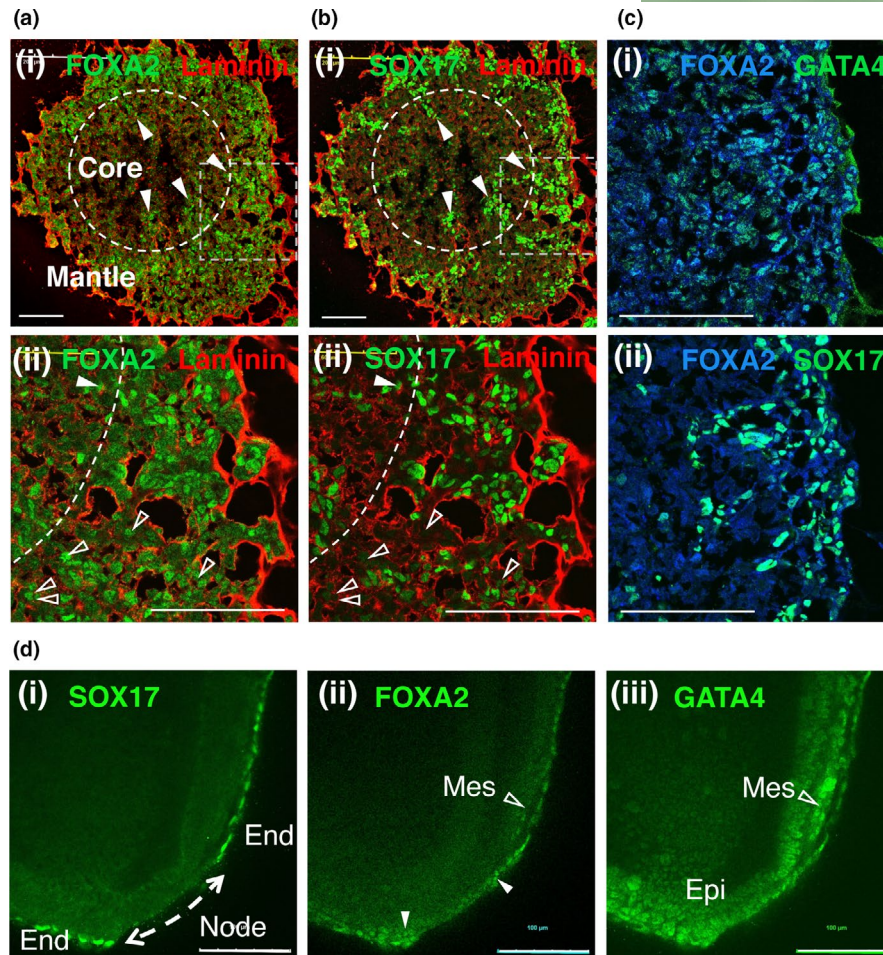


FIGURE 5 Relationship of SOX17-expressing cells with expression of FOXA2 and GATA4 in comparison with mouse embryos. (a) to (c) Representative data using a D6-Mt aggregate of a slightly advanced stage than those shown in Figure 5b,c. A rough boundary between the core and mantle zones, indicated by the broken circle, was drawn as a radial contour or the zone free from thick laminin immunostaining. (a) Comparison of laminin immunostaining and distribution of FOXA2-expressing cells with two distinct expression levels. (b) Comparison of laminin immunostaining and distribution of SOX17-expressing cells in the same section as in (a). (i) A section showing the entire region of a cryosection. In the core zone the cells with a low level of FOXA2 expression are abundant, but in the mantle zone, cells with a high level of FOXA2 expression predominated. In the core zone, some populations expressing a relatively high level of FOXA2 and a high level of SOX17 formed stream-like cell clusters, which are indicated by arrowheads. (ii) A high power view of the section area indicated by the broken square in (i). Virtually all cells in this area expressed FOXA2, and the cells expressing FOXA2 at a low level had the TF in both the nucleus and cytoplasm. SOX17-expressing cells also expressed a high level of FOXA2, but a small fraction of high FOXA2-expressing cells lacked SOX17 expression, some examples of which are indicated by open arrowheads. (c) A section area analogous to (a)(ii) and (b)(ii) of the same aggregate, but at a different section level, comparing expression of FOXA2, GATA4, and SOX17. (i) Comparison of FOXA2 and GATA4 expression, indicating that expression of these TFs is shared in the cells of this area. (ii) Comparison of FOXA2 and SOX17 expression. A corollary from the comparison of (c) with (a)(ii) and (b)(ii) is that the SOX17-expressing cells represent a specific subpopulation of the FOXA2/GATA4-expressing population. (d) An E7.5 mouse embryo stained for (i) SOX17, (ii) FOXA2, and (iii) GATA4. An optical section around the node is shown. Anterior is to the right. (i) SOX17-marked definitive endoderm (End) developed outside the node region. (ii) High FOXA2 expression occurs in the SOX17-expressing endoderm and also endoderm-proximal cells (arrowheads), which presumably represent pre-endoderm still in the migratory phase of the gastrulation. Low FOXA2 expression occurs in the mesodermal cells (Mes, open arrowhead). (iii) GATA4 was expressed in all endoderm, pre-endoderm, node, mesoderm, and also epiblast (Epi) of this developmental stage. Bars, 100 μm

The i22 aggregate at day 3 (D3) in floating culture before embedding in Matrigel expressed POU5F1 and SOX2 in the nuclei, and also E-cadherin at intercellular junctions in virtually all cells (Figure 4a), indicating that the cells are still in the epiblast state. Nevertheless, the cells appeared to be primed for endoderm development, because of the widespread *FoxA2*-EGFP expression and more sporadic expression of SOX17 (Figure 2b).

After 3 days of placing the aggregates in Matrigel (D6), the D6-Mt aggregates were surrounded by a mesh of laminin-containing matrices (Figure 4b(i)), which were absent in D6-FF cell aggregates (see Figure 7b). In the internal core region of the aggregates free from laminin-containing meshes (Figure 4b), a fraction of cells expressed SOX17 and formed small clusters, although they still expressed POU5F1 and SOX2 (Figure 4c), suggesting that they

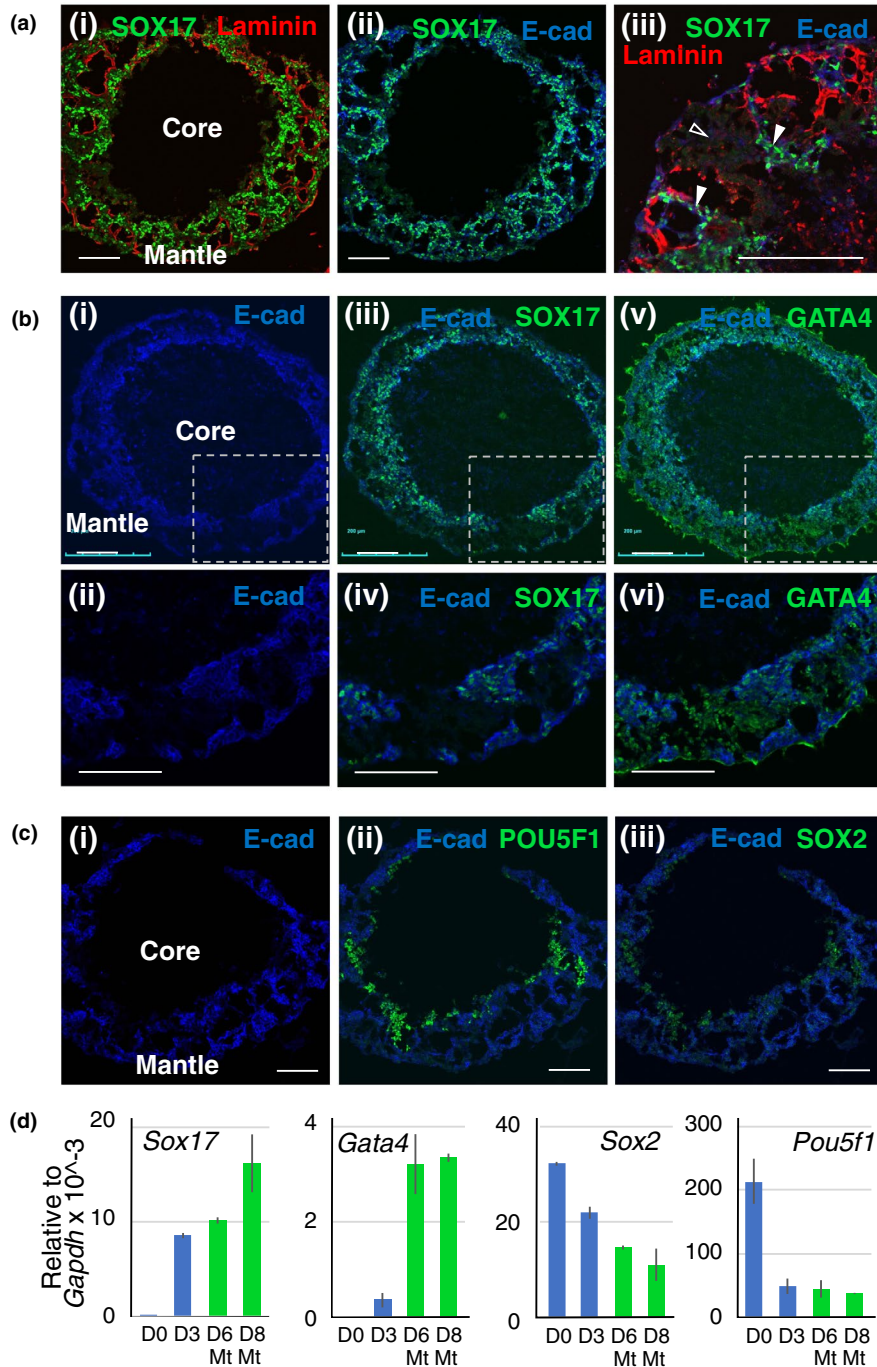
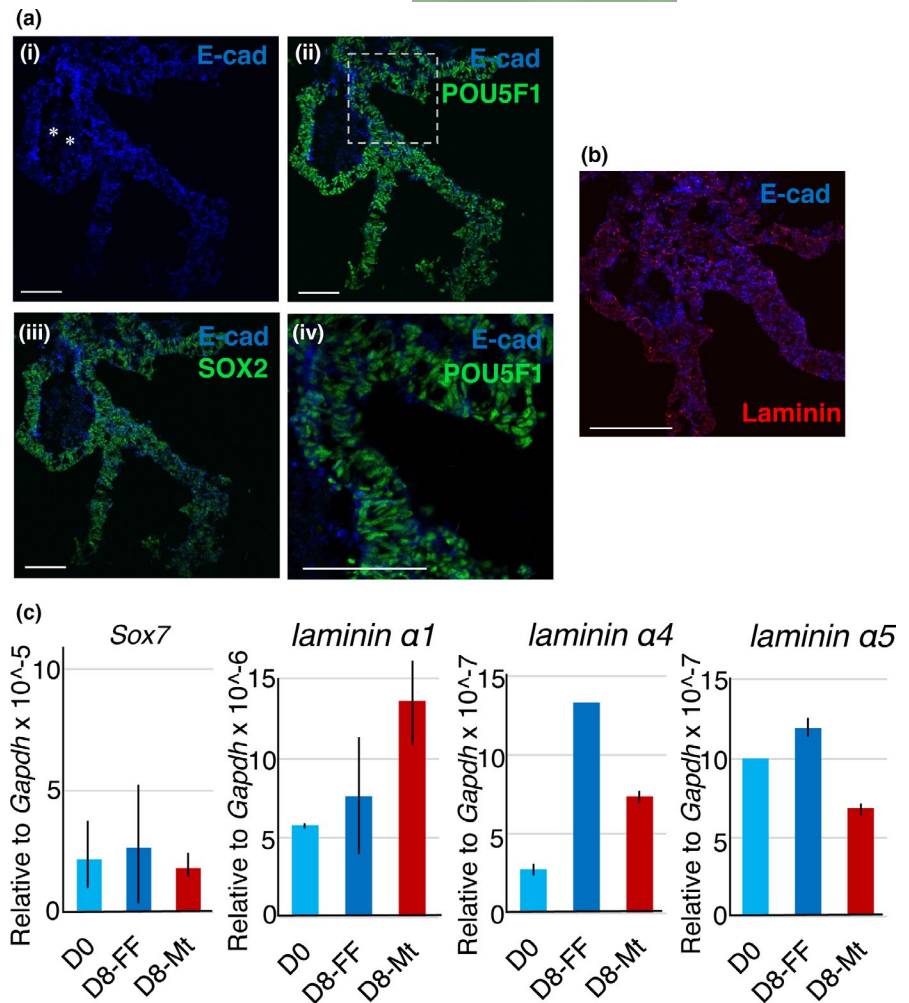


FIGURE 6 Segregations of cell populations marked by TF expression in D8-Mt aggregates. (a) A D8-Mt aggregate derived from i22 cells stained for laminin, SOX17 and E-cadherin. The core zone of the aggregate virtually lacked cells. (i) Laminin and SOX17, and (ii) SOX17 and E-cadherin co-staining data, showing that SOX17- and E-cadherin-expressing epitheloid cell clusters were distributed between the ducts/spherical cavity formed by the laminin-rich matrix. However, SOX17-nonexpressing cells were also present. (iii) A large power view of a part of an analogous section showing that the SOX17/E-cadherin-negative cell cluster (open arrowhead), filling the gap between the epitheloid clusters (arrowheads). (b) Spatial relationship between SOX17-expressing cells and GATA4-expressing cells in a D8-Mt aggregate. (i, ii) Distribution of E-cadherin in the entire aggregate (i) and a high power view of the area indicated by the broken rectangle. (iii, iv) Superimposition of SOX17 and E-cadherin immunofluorescence, indicating coincidence of SOX17-expressing and E-cadherin expressing cells. (v, vi) Superimposition of GATA4 and E-cadherin immunofluorescence, indicating that all cells expressed GATA4, regardless of SOX17/E-cadherin expression. Overall, SOX17/E-cad-expressing epitheloid cell population and GATA4-only cell population segregated each other in the D8-Mt aggregates. (c) A section of a D8-Mt aggregate stained for (i) POU5F1 and E-cadherin or (ii) SOX2 and E-cadherin, indicating POU5F1/SOX2-expressing, E-cadherin negative cells still exist in the aggregate, similar to those observed in the outer area of the D6-Mt core zone (Figure 4c). Bars, 100 μ m. (d) Changes in expression levels of *Sox17*, *Gata4*, *Sox2* and *Pou5f1* between D6-Mt and D8-Mt aggregates examined by RT-qPCR analysis. RNA samples from the same experimental batch as for histological analysis of D6-Mt to D8-Mt aggregates were analyzed in comparison with those used for D0 and D3 aggregates in Figure 3. The large difference of the *Gata4* level at D3-Mt compared to Figure 3 presumably reflects an asynchrony of molecular events between different batches of aggregate samples

FIGURE 7 Characterization of D8-FF aggregates consisting of laminated epitheloid tissues. (a) A cross section stained for E-cadherin, SOX2, and POU5F1. (i) Distribution of E-cadherin. Asterisks indicate the fluorescent signals derived from remnants of dead cells. (ii) Overlap of E-cadherin and POU5F1 expression. (iii) Overlap of E-cadherin and SOX2. (iv) A high power view of the area in the rectangle in (ii), which confirms the coexpression of E-cadherin and POU5F1. (b) Comparison of the distribution of E-cadherin and laminin. Bars, 100 μm . (c) Comparison of expression levels of *Sox7* and *laminins* $\alpha 1$, $\alpha 4$, and $\alpha 5$ in i22 EpiSCs (D0), D8-FF and D8-Mt aggregates by RT-qPCR analysis. The transcript levels are shown relative to *Gapdh* level, and error bars indicate the data range of two samples



represent endoderm-ready epiblast cells. In the outer mantle zone containing laminin matrices, the cells expressing SOX17 but without POU5F1 or SOX2 were distributed (Figure 4b,c). It was noted that the majority of SOX17-expressing cells in the mantle zone had lost E-cadherin expression, suggesting that the SOX17-positive cells in the core zone had migrated into the laminin-rich mantle zone. These tissue organizations were reminiscent of the gastrulation process to produce endoderm precursors *in vivo*, where endoderm precursors in the epiblast layer pass through the basement membrane and assume a transient migratory state before reforming endodermal epithelial sheet (Arnold et al., 2008; Nowotschin et al., 2019).

In the mantle zone, some of the SOX17-expressing cells clustered in an elongated form and expressed E-cadherin at a high level, suggesting the development into the definitive endoderm cell state (Figure 4b; Tada et al., 2005). In some cases, the clusters with strong SOX17 and E-cadherin expression but without POU5F1 or SOX2 traversed the core/mantle boundary (Figure 4b,c, broken rectangles). It is possible that these represent clusters of SOX17-expressing cells streaming out from the core zone. The data suggest that once the frontier cells started to develop into the definitive endoderm state, the remaining cell population also developed into the definitive endoderm. These observations overall suggested the following steps:

once the SOX17/SOX2/POU5F1-expressing, endoderm-primed epiblast cells interact with the laminin-rich matrix, they enter into the migratory phase losing E-cadherin expression. These migratory cells then settle on the matrix and form E-cadherin-expressing epithelial cell groups of definitive endoderm.

3.5 | SOX17-expressing cells represent a subpopulation of FOXA2/GATA4-expressing population in the Matrigel-embedded aggregates

The relationship of SOX17 expression with the expression of FOXA2 and GATA4 in Matrigel-embedded aggregates was investigated using aggregates of the D6-Mt group, but with features of slightly more advanced stage than the one shown in Figure 4.

The FOXA2-expressing cell population occupied the external side of the core zone and the mantle zone (Figure 5a,b(i,ii)), where two subpopulations were distinguished: (1) The population expressing a relatively high level of FOXA2 and a high level of SOX17, forming a stream-like cell clusters continuing from the external core zone into the mantle zone (arrowheads), suggesting that the cells are migrating to form the definitive endoderm in the outer zone. These cells also express GATA4 (Figure 5c, compare (i)

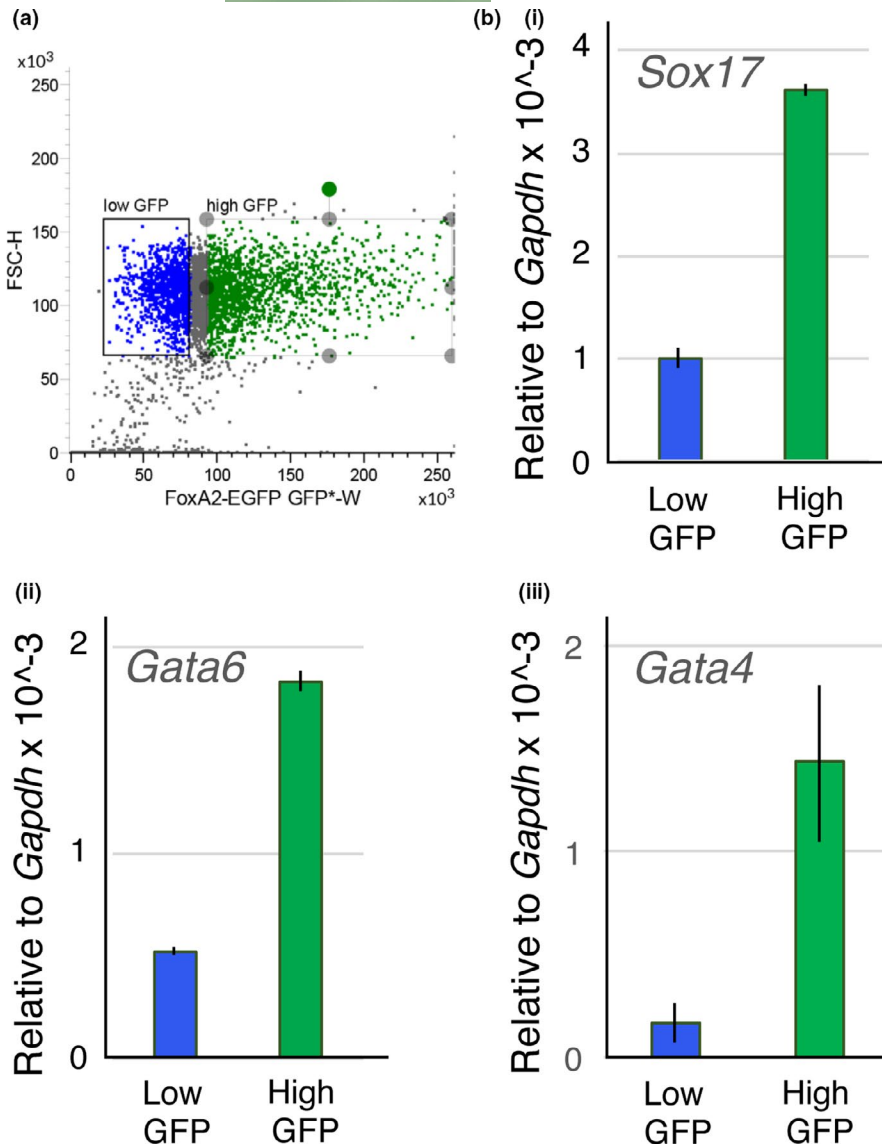


FIGURE 8 Fractionation of i22-derived cells in aggregates using *Foxa2*-EGFP expression level as a gate for FACS. Two independently cultured i22 cells in D6-Mt aggregation culture were dissociated into single cells and subjected to FACS. (a) FACS plot of a representative sample. The abscissa indicates the GFP fluorescence level, whereas the ordinate indicates the forward scattering level. From 20,000 cells applied to FACS Melody with the gate setting shown, approximately 2,000 cells were collected in both high GFP and low GFP fractions. (b) The fractionated cells were subjected to RT-qPCR analysis of *Sox17*, *Gata4*, and *Gata6* expression. The ordinate indicates the relative transcript level compared to 10⁻³ of *Gapdh*, the vertical bars indicate the average of the biological duplicate as indicated above, and the error bars indicate the data range. Note that expression levels of *Sox17*, *Gata4* and *Gata6* were all higher in the high GFP fraction

GATA4 and (ii) SOX17). A small fraction of cells with high FOXA2-expressing cells lacked SOX17 expression (Figure 5a,b(ii), open arrowheads), which may represent a premature state before the FOXA2/SOX17 double-positive endoderm precursor state. (2) The remaining population expressing a moderate level of FOXA2 and GATA4 (Figure 5a(ii),c(i)). GATA4 was expressed virtually all cells expressing FOXA2 regardless of the expression level of FOXA2 or SOX17 expression (Figure 5c(i,ii)).

Overall, SOX17-expressing cells in D6-Mt aggregates are likely on the way of definitive endoderm development, as a subpopulation of FOXA2/GATA4-expressing cells. Compared with the tissues that developed in E7.5 mouse embryos (Figure 5d), SOX17-expressing cells (also expressing FOXA2 and GATA4) represent the endoderm precursors, and those expressing high FOXA2 but without SOX17 presumably represent those cells migrating down but before settling in the endodermal layer (Figure 5d(ii), arrowheads). The cells with expression of GATA4 and low-level FOXA2 appear to correspond to the mesodermal cells at this stage of mouse embryos (Figure 5d(ii,iii), open arrowhead).

3.6 | Segregation of SOX17/GATA4-high/E-cadherin-expressing epitheloid cell clusters and GATA4-low populations

After culturing in Matrigel for 5 days (D8-Mt), the aggregates further increased in size, and had a conspicuous mantle zone, whereas the core zone contained remnant dead cells or even became hollow, suggesting that a large fraction of cells that were in the core zone of D6-Mt aggregates migrated out into the mantle zone (Figure 6).

In the thick mantle zone, the SOX17-expressing cells formed large epitheloid cell clusters (thickness of a few cells) expressing E-cadherin, which were often found on tubular structures made of laminin-containing matrices (Figure 6a(i,ii)). However, it was noted that the mantle zone also contained other types of cells (open arrowhead in Figure 6a(iii) between SOX17-expressing cells (arrowheads in (Figure 6a(iii)).

Comparison of E-cadherin-, SOX17-, and GATA4-expressing cells indicated two segregating major populations of cells (Figure 6b):

first, those highly expressing SOX17, GATA4, and E-cadherin to form epitheloid cell clusters, which represent definitive endoderm; and second those expressing a lower level of GATA4 without accompanying SOX17 or E-cadherin expression and filling the spaces in between the SOX17-expressing clusters. Compared with TF expression patterns in D6-Mt aggregates and E7.5 embryos (Figure 5), the former population corresponded to the SOX17-expressing endodermal cells, which were accompanied by various levels of GATA4 expression, and the latter to the mesodermally positioned GATA4 single positive population, putative cardiac precursors.

As the third population, POU5F1- and SOX2-expressing cells forming loose clusters were also found as a part of GATA4-expressing population (Figure 6c). These cells may represent an epiblast state, but lacked high E-cadherin expression. Presumably these cells were carryover of the gastrulation-ready, low E-cadherin epiblast, which were observed in the outer region of the core zone in D6-Mt aggregates (Figure 4c).

We investigated possible changes in the expression levels of TF genes *Sox17*, *Gata4*, *Sox2*, and *Pou5f1* during D6-Mt and D8-Mt period when different cell populations completed their mutual sorting (Figure 6d). Only moderate changes were observed in the expression levels of these TFs, some rise with *Sox17* and *Gata4* and decrease with *Sox2* and *Pou5f1*. This observation indicates that the spatially separate cell groups, SOX17+/E-cadherin+, GATA4+/E-cadherin-, and SOX2+/POU5F1+/E-cadherin-, were formed without much change in the expression levels of these TFs.

3.7 | FF EpiSC aggregation culture selects for epiblast cells

In FF aggregates cultured longer than 3 days, the expression of *Foxa2*-EGFP (Figure 2c) or *Sox17* expression was lost (Figure 3c), and the aggregates consisted of laminated epitheloid tissues strongly expressing POU5F1, SOX2, and E-cadherin, indicating that the majority of cells in the aggregates consisted of epiblast cells (Figure 7). It was also noted that the epitheloid epiblast tissues were accompanied by remnants of dead cells (Figure 7(i), asterisks). The simple aggregation in the ordinary EpiSC culture medium seems to provide a condition strongly in favor of epiblast states but selecting against other cell types.

We also examined the possible development of some neural characteristics in i22 cell aggregates in long term culturing (D6 and D8) by immunostaining. We observed no expression of neural TFs, POU3F1 (OCT6), POU3F2 (BRN2), or PAX6, in the aggregates, regardless of Matrigel embedding (data not shown).

3.8 | Additional characterization of D8-Mt aggregates by comparison with D8-FF aggregates

In the above analyses, we used *Sox17*/SOX17 expression as a marker for the definitive endoderm precursors. However, the

extraembryonic endoderm also expresses *Sox17*, but is distinct for its expression of *Sox7* together. The definitive endoderm nature of the SOX17-expressing cells in D8-Mt aggregates was confirmed by RT-qPCR analysis using D8-FF as a control, showing no activation of extraembryonic endoderm-specific *Sox7* expression (Figure 7c).

At 5 days in Matrigel (D8-Mt), the laminin meshes appeared to be more organized into duct-like structures (Figure 6a), compared with D6-Mt aggregates (Figures 4b and 5a). D8-FF aggregates did not have such thick laminin meshwork, but had a low-level laminin finely distributed along cellular boundaries, similar to those observed in the core region of D6-Mt aggregates (Figures 4b and 5a,b). We examined the possibility of activation of laminin synthesis via placing i22 cell aggregates in Matrigel by comparing D8-Mt and D8-FF aggregates. Results of the RT-qPCR analysis indicated that the expression levels of *laminin α1*, *α4*, or *α5* were very low, comparable to EpiSCs, and similar (within two-fold differences) between D8-Mt and D8-FF aggregates (Figure 7c). Therefore, at least the majority of laminin-rich matrices in the mantle zone were derived from Matrigel. The cells appeared to reshape the distribution of Matrigel-derived matrices, presumably owing to possession of some proteolytic activity to degrade extracellular matrices, and/or by integrating endogenously expressed laminins into the matrices.

3.9 | Isolation of *Foxa2*-EGFP-expressing cell population by fluorescence-activated cell sorting

Given that the majority of SOX17-expressing and/or GATA4-expressing cells are FOXA2-positive, as shown by immunofluorescence (Figure 5), we attempted to isolate these cell populations by fluorescence-activated cell sorting (FACS) using *Foxa2*-EGFP fluorescence for sample gating (Figure 8a).

In an experiment shown in Figure 8a, the dissociated i22 cells from D6-Mt aggregates were sorted as high and low EGFP-expressing populations using a FACS equipment; high and low EGFP-expressing populations were collected with ratios between 1 and 1.5. RNAs were isolated from these sorted cell populations and analyzed for transcript levels by using RT-qPCR. As shown in Figure 8b, *Sox17*, *Gata6*, and *Gata4* transcript levels were several fold higher in the high GFP fraction, indicating the feasibility of isolation of endodermal/cardiac precursors, for further analyses or for culturing as less heterogeneous cell populations than the original aggregates.

4 | DISCUSSION

4.1 | Development of definitive endodermal cells from EpiSCs, utilizing their cell-autonomous developmental potential

In this study, we have established an experimental condition to derive definitive endodermal cells expressing SOX17 from EpiSCs,

utilizing their cell-autonomous developmental potential and their interaction with exogenously supplied laminin-rich matrices in the form of Matrigel, which mimic the cellular events that occur in developing embryos. Firstly, we have shown that aggregation of EpiSCs primes their development into endodermal and other somatic lineages, and placing the aggregates in Matrigel promoted endodermal development involving cell migration phase with eventual settling into the space in laminin-rich matrices. Secondly, we have also shown that the SOX17-expressing cells develop as a subpopulation of GATA4-expressing cells, which presumably represent cardiac precursors. These are schematically shown in Figure 9a,b, respectively. In the following chapters, we summarize some details of these processes, which can be extracted from data shown in the Section 3.

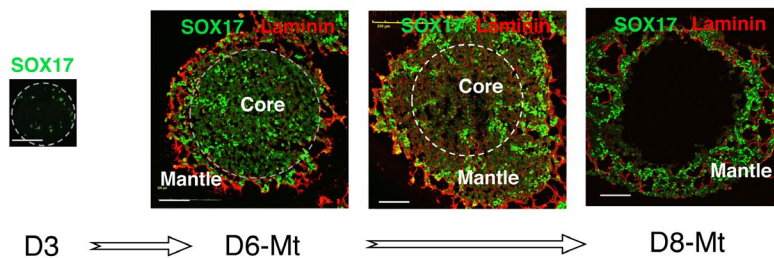
4.2 | Activation of somatic developmental potentials in EpiSC aggregates

To facilitate the detection of endodermal development, we established a new EpiSC line i22, which expresses nuclearly localized EGFP when the *Foxa2* gene is activated (*Foxa2*-EGFP). Under

the spreading culture condition, the *Foxa2*-EGFP expression in i22 EpiSCs was almost silent (Figure 2a). However, *Foxa2*-EGFP expression was activated in 2 days from the start of floating culture (Figure 2). Immunohistological analysis (Figure 2) and RT-qPCR analysis (Figure 3) indicated that the genes representing early somatic lineage development, *Sox17* (expressed in definitive endoderm precursor), *Gata4* (expressed in endodermal and cardiac precursors), and *Bra* (expressed in node, notochord and prechordal plate) were all activated, although these cells still expressed POU5F1 and SOX2 (Figures 3a and 4a), suggesting that the change from adherence culture condition to cell aggregates primed the somatic development of EpiSCs, yet in 3 days of floating culture was not sufficient for cells to enter somatic development stages.

Prolonged free-floating (FF) aggregate cultures, however, downregulated *Foxa2*-EGFP expression (Figure 2c) and also the expression of *Sox17*, *Gata4*, and *Bra* (Figure 3b), while sustaining the expression of POU5F1 and SOX2 (Figures 3a and 7a). Histological examination of FF aggregates of longer than 3 days of culturing indicated that cell aggregates were not spherical anymore, and consisted of POU5F1- and SOX2-expressing epitheloid laminae, likely epiblast cells, which were accompanied by numerous dead cells (Figure 7a). These observations suggested that simple cell

(a) Changes in the distribution of SOX17-expressing cells in the aggregates



(b) Changes in the overlap and segregation of cell groups expressing various sets of TFs

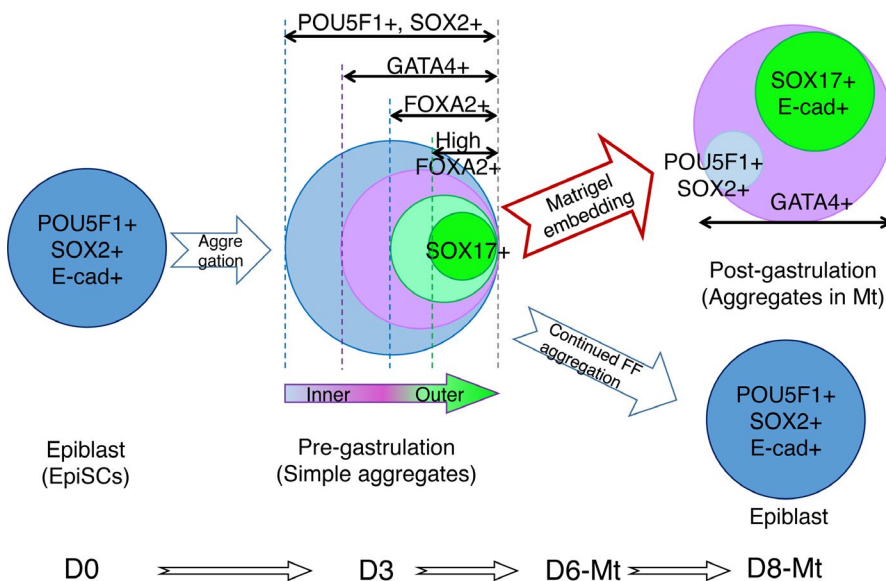


FIGURE 9 Summary of two major observations made in this study. (a) Changes in the distribution of SOX17-expressing cells in the EpiSC aggregates. The SOX17-expressing cells initially arises at scattered positions in simple FF aggregates (D3). Embedding the aggregates in laminin-rich Matrigel increased the fraction of SOX17-expressing endoderm precursor cells by D6. These SOX17-expressing cells migrated out in the laminin-rich mantle zone, often forming streams of cells, and eventually settled in the mantle zone forming epitheloid endodermal tissues. (b) Changes in the overlap and segregation of cell groups expressing various combinations of TFs. The scheme in the middle indicates the state of a D3 aggregate, where right and left positioning of circles indicates the tendency of the distribution of the type of cells more outer and inner positions, respectively, in an aggregate. E-cadherin expression at this stage is complex, and is not shown in the scheme. The schemes on the right indicate the states of D8 aggregates, D8-Mt (top) and D8-FF (bottom)

aggregates in the maintenance culture medium were not compatible with somatic development and/or viability of somatic cells. The observation even suggested the feasibility of stable maintenance of EpiSCs as floating cell aggregates.

4.3 | Activation of endodermal developmental program in EpiSC aggregates with the supply of laminin-rich extracellular matrix

In normal embryos at the stage prior to gastrulation, the epiblast is underlain by the extracellular matrix rich in laminin (Futaki, Nakano, Kawasaki, Sanzen, & Sekiguchi, 2019). The endoderm precursors in the epiblast layer first assume a migratory state (Arnold et al., 2008; Nowotschin et al., 2019), then destabilize the matrix via protease secretion in a FOXA2-dependent manner, and finally migrate through the matrix down to the bottom layer to form an epithelial endoderm layer (Burtscher & Lickert, 2009; Viotti et al., 2014). We reasoned that an exogenous supply of laminin-rich basement membrane components, by embedding the EpiSC aggregates in Matrigel, may provide the condition for the endoderm lineage-primed EpiSCs to enter the somatic development process.

Embedded and suspended in Matrigel, the EpiSC aggregates indeed continued to show *Foxa2*-EGFP expression in the prolonged culture period (Figure 2c), and exhibited sequential activation of TF genes involved in endoderm development (*Eomes*, *Gsc*, and *Sox17*) and cardiac development (*Mesp1*, *Gata6*, and *Gata4*; Figure 3c,d). At the histological level, the aggregates spending 3 days in Matrigel (D6-Mt), comprised core and mantle zones (Figure 4). The core zone consisted of POU5F1-, SOX2-, and E-cadherin-expressing cells, many of which expressed a moderate level of GATA4 and less frequently SOX17, similar to those in 3-day simple aggregates. However, the POU5F1- and SOX2-expressing cells at the periphery of the core zone downregulated E-cadherin expression, suggesting that these cells were prepared for migrating out into the mantle zone.

At an early stage of D6-Mt aggregates, shown in Figure 4b,c, the mantle zone was formed in the external meshwork of the matrices, being colonized by cells expressing GATA4 and/or SOX17. Most notably, cells in the mantle zone were mostly free from E-cadherin, in contrast to the core zone cells expressing E-cadherin, suggesting that a significant fraction of mantle zone cells are in the migratory state. A fraction of SOX17-expressing cells in the mantle zone formed cell clusters and expressed E-cadherin, possibly indicating the initiation of epithelial endoderm formation.

The next step of the developmental process in Matrigel-embedded aggregates is represented by the aggregates shown in Figure 5. There, the mantle zone was expanded, and a fraction of core zone cells expressing a high level of FOXA2 and SOX17 formed a cell cluster that appeared to be streaming into the mantle zone (Figure 5a,b). All mantle zone cells expressed GATA4 and FOXA2, but were clearly classified into two groups according to the expression level of FOXA2. The majority of high

FOXA2-expressing group cells also expressed SOX17, suggesting that cells with moderate GATA4 and high FOXA2 expression were pre-endodermal precursors.

After further development of the aggregates in Matrigel, represented by a D8-Mt sample (Figure 6), the mantle zones of cell aggregates were very rich in cells that were distributed along with laminin-rich matrices (Figure 6), whereas the core zone was almost vacant with live cells (Figure 6), presumably as a consequence of active cell migration out of the core zone and/or of nutritional deficiency in the deep core zone of enlarged aggregates. In the mantle zone, SOX17- and E-cadherin expressing definitive endoderm cells formed thick epitheloid cell clusters in association with laminin-rich matrices organized into tubular structures. The cells expressing only GATA4 and devoid of E-cadherin filled the remaining spaces between the matrix tubes in the mantle zone. On the internal side of the mantle zone resided epiblast-like cells expressing POU5F1 and SOX2, but without high E-cadherin expression. Thus, all three components of post-gastrulation embryos were present at this stage of i22 cell aggregates, namely the definitive endoderm expressing SOX17, mesoderm expressing GATA4 only, and putative gastrulation-ready epiblast expressing POU5F1 and SOX2 in addition to GATA4. The cellular changes starting from the epiblast leading to the definitive endoderm formation, as observed in the Matrigel-embedded aggregates (Figures 4–6) and having correspondences with gastrulating embryos (Figure 5d), are presented in a schematic layout in Figure 9.

In summary, during 3–5 days in Matrigel (D6-Mt to D8-Mt), as shown in the specimens in Figures 4–6, cells in the aggregates developed into different populations found around the node in mouse embryos during endoderm-producing gastrulation (Figure 5d). Moreover, these cells appeared to develop into endoderm and cardiac precursors, via a migratory state losing E-cadherin expression and passing through the laminin-rich matrices. In this way, the early stages of endoderm development were nicely modeled in EpiSC aggregates with the supply of extracellular matrices. This study also highlighted the importance of intercellular signaling in the epiblast, which is elicited via the interaction of cells with the basement membrane. Moreover, experimental manipulation of TF expression and/or signaling systems in the aggregates, which may affect endoderm development, will provide crucial information concerning cellular regulations leading to endoderm development.

4.4 | The possibility of precursor sharing by the endodermal and cardiac lineages

It has been shown that TFs GATA4 and GATA6 are involved in the development of both the endoderm precursors (Bossard & Zaret, 1998; Fisher et al., 2017; Molkenin, 2000; Simon et al., 2018; Teo et al., 2011) and cardiac precursors (Charron & Nemer, 1999; Kuo et al., 1997; Molkenin et al., 1997; Zhao et al., 2008). Despite the expression of GATA4 and GATA6 is common to the endodermal and cardiac lineages, their expression in different lineages have been regarded as separate events.

In this study, we showed that FOXA2/SOX17-expressing endoderm precursor cells develop as a subpopulation, rather than as a separate population, of GATA4-expressing cells that include cardiac precursors (Figures 2, 5, 6, and 9). This observation raised the possibility that endodermal and cardiac lineages develop from the same precursor pool. We also found that early-stage TF genes involved in the endodermal lineage, i.e., *Eomes*, *Gsc*, and *Sox17*, and those involved in the cardiac lineage, i.e., *Mesp1*, *Gata6*, and *Gata4* were expressed in sequence and in analogous time courses in EpiSC aggregates followed by Matrigel embedding. Consistently, it was indicated in an ESC model that EOMES activates *Mesp1*, thereby initiating the cardiac lineage development, in addition to the activation of endodermal lineage (van den Aamele et al., 2012). The earlier observations indicating that functional cooperation of GATA4 and FOXA2 opens up the endoderm developmental pathway (Bossard & Zaret, 1998; Cirillo et al., 2002; Zaret, 1999) also support the model in which endoderm precursors arise as a subpopulation of cardiac precursors. Moreover, a previous study demonstrated that turnoff of Wnt signaling via conditional β -catenin knockout in the established endodermal tissue results in development of ectopic cardiac tissues (Lickert et al., 2002), underscoring a strong kinship between endodermal and cardiac lineages. The experimental system reported in this study will also be useful in determining relationships between the endodermal and cardiac lineages.

ACKNOWLEDGMENTS

We thank Hiroshi Sasaki for granting the use of the *Foxa2-Egfp* knockin mice. This study was supported by Grants-in-Aid for Scientific Research, JP19K16184 to MT and JP17H03688 to HK from MEXT Japan, Private University Research Branding Project of MEXT, and Kyoto Sangyo University Research Fund for Institute for Protein Dynamics.

ORCID

Hisato Kondoh  <https://orcid.org/0000-0002-3609-7014>

REFERENCES

- Arnold, S. J., Hofmann, U. K., Bikoff, E. K., & Robertson, E. J. (2008). Pivotal roles for eomesodermin during axis formation, epithelium-to-mesenchyme transition and endoderm specification in the mouse. *Development*, *135*, 501–511. <https://doi.org/10.1242/dev.014357>
- Bossard, P., & Zaret, K. S. (1998). GATA transcription factors as potentiators of gut endoderm differentiation. *Development*, *125*, 4909–4917.
- Brons, I. G., Smithers, L. E., Trotter, M. W., Rugg-Gunn, P., Sun, B., de Sousa, C., ... Vallier, L. (2007). Derivation of pluripotent epiblast stem cells from mammalian embryos. *Nature*, *448*, 191–195. <https://doi.org/10.1038/nature05950>
- Burtscher, I., & Lickert, H. (2009). *Foxa2* regulates polarity and epithelialization in the endoderm germ layer of the mouse embryo. *Development*, *136*, 1029–1038. <https://doi.org/10.1242/dev.028415>
- Charron, F., & Nemer, M. (1999). GATA transcription factors and cardiac development. *Seminars in Cell & Developmental Biology*, *10*, 85–91. <https://doi.org/10.1006/scdb.1998.0281>
- Cirillo, L. A., Lin, F. R., Cuesta, I., Friedman, D., Jarnik, M., & Zaret, K. S. (2002). Opening of compacted chromatin by early developmental transcription factors HNF3 (FoxA) and GATA-4. *Molecular Cell*, *9*, 279–289. [https://doi.org/10.1016/s1097-2765\(02\)00459-8](https://doi.org/10.1016/s1097-2765(02)00459-8)
- Fisher, J. B., Pulakanti, K., Rao, S., & Duncan, S. A. (2017). GATA6 is essential for endoderm formation from human pluripotent stem cells. *Biology Open*, *6*, 1084–1095. <https://doi.org/10.1242/bio.026120>
- Futaki, S., Nakano, I., Kawasaki, M., Sanzen, N., & Sekiguchi, K. (2019). Molecular profiling of the basement membrane of pluripotent epiblast cells in post-implantation stage mouse embryos. *Regenerative Therapy*, *12*, 55–65. <https://doi.org/10.1016/j.reth.2019.04.010>
- Imuta, Y., Kiyonari, H., Jang, C. W., Behringer, R. R., & Sasaki, H. (2013). Generation of knock-in mice that express nuclear enhanced green fluorescent protein and tamoxifen-inducible Cre recombinase in the notochord from *Foxa2* and *T* loci. *Genesis*, *51*, 210–218. <https://doi.org/10.1002/dvg.22376>
- Iwafuchi-Doi, M., Matsuda, K., Murakami, K., Niwa, H., Tesar, P. J., Aruga, J., ... Kondoh, H. (2012). Transcriptional regulatory networks in epiblast cells and during anterior neural plate development as modeled in epiblast stem cells. *Development*, *139*, 3926–3937. <https://doi.org/10.1242/dev.085936>
- Kanai-Azuma, M., Kanai, Y., Gad, J. M., Tajima, Y., Taya, C., Kurohmaru, M., ... Hayashi, Y. (2002). Depletion of definitive gut endoderm in *Sox17*-null mutant mice. *Development*, *129*, 2367–2379.
- Kinoshita, M., Shimosato, D., Yamane, M., & Niwa, H. (2015). *Sox7* is dispensable for primitive endoderm differentiation from mouse ES cells. *BMC Developmental Biology*, *15*, 37. <https://doi.org/10.1186/s12861-015-0079-4>
- Kuo, C. T., Morrisey, E. E., Anandappa, R., Sigrist, K., Lu, M. M., Parmacek, M. S., ... Leiden, J. M. (1997). GATA4 transcription factor is required for ventral morphogenesis and heart tube formation. *Genes & Development*, *11*, 1048–1060. <https://doi.org/10.1101/gad.11.8.1048>
- Lickert, H., Kutsch, S., Kanzler, B., Tamai, Y., Taketo, M. M., & Kemler, R. (2002). Formation of multiple hearts in mice following deletion of beta-catenin in the embryonic endoderm. *Developmental Cell*, *3*, 171–181. [https://doi.org/10.1016/s1534-5807\(02\)00206-x](https://doi.org/10.1016/s1534-5807(02)00206-x)
- Matsuda, K., & Kondoh, H. (2014). *Dkk1*-dependent inhibition of Wnt signaling activates *Hesx1* expression through its 5' enhancer and directs forebrain precursor development. *Genes to Cells*, *19*, 374–385. <https://doi.org/10.1111/gtc.12136>
- Matsuda, K., Mikami, T., Oki, S., Iida, H., Andrabi, M., Boss, J. M., ... Kondoh, H. (2017). ChIP-seq analysis of genomic binding regions of five major transcription factors highlights a central role for *ZIC2* in the mouse epiblast stem cell gene regulatory network. *Development*, *144*, 1948–1958. <https://doi.org/10.1242/dev.143479>
- Mccauley, H. A., & Wells, J. M. (2017). Pluripotent stem cell-derived organoids: Using principles of developmental biology to grow human tissues in a dish. *Development*, *144*, 958–962. <https://doi.org/10.1242/dev.140731>
- Molkentin, J. D. (2000). The zinc finger-containing transcription factors GATA-4, -5, and -6. Ubiquitously expressed regulators of tissue-specific gene expression. *Journal of Biological Chemistry*, *275*, 38949–38952. <https://doi.org/10.1074/jbc.R000029200>
- Molkentin, J. D., Lin, Q., Duncan, S. A., & Olson, E. N. (1997). Requirement of the transcription factor GATA4 for heart tube formation and ventral morphogenesis. *Genes & Development*, *11*, 1061–1072. <https://doi.org/10.1101/gad.11.8.1061>
- Nowotschin, S., Hadjantonakis, A. K., & Campbell, K. (2019). The endoderm: A divergent cell lineage with many commonalities. *Development*, *146*, 150920. <https://doi.org/10.1242/dev.150920>
- Saga, Y., Miyagawa-Tomita, S., Takagi, A., Kitajima, S., Miyazaki, J., & Inoue, T. (1999). *MesP1* is expressed in the heart precursor cells and

- required for the formation of a single heart tube. *Development*, 126, 3437–3447.
- Schindelin, J., Arganda-Carreras, I., Frise, E., Kaynig, V., Longair, M., Pietzsch, T., ... Cardona, A. (2012). Fiji: An open-source platform for biological-image analysis. *Nature Methods*, 9, 676–682. <https://doi.org/10.1038/nmeth.2019>
- Simon, C. S., Zhang, L., Wu, T., Cai, W., Saiz, N., Nowotschin, S., ... Hadjantonakis, A. K. (2018). A Gata4 nuclear GFP transcriptional reporter to study endoderm and cardiac development in the mouse. *Biology Open*, 7, 36517. <https://doi.org/10.1242/bio.036517>
- Simunovic, M., & Brivanlou, A. H. (2017). Embryoids, organoids and gastruloids: New approaches to understanding embryogenesis. *Development*, 144, 976–985. <https://doi.org/10.1242/dev.143529>
- Sugimoto, M., Kondo, M., Koga, Y., Shiura, H., Ikeda, R., Hirose, M., ... Abe, K. (2015). A simple and robust method for establishing homogeneous mouse epiblast stem cell lines by wnt inhibition. *Stem Cell Reports*, 4, 744–757. <https://doi.org/10.1016/j.stemcr.2015.02.014>
- Sumi, T., Oki, S., Kitajima, K., & Meno, C. (2013). Epiblast ground state is controlled by canonical Wnt/beta-catenin signaling in the post-implantation mouse embryo and epiblast stem cells. *PLoS ONE*, 8, e63378. <https://doi.org/10.1371/journal.pone.0063378>
- Tada, S., Era, T., Furusawa, C., Sakurai, H., Nishikawa, S., Kinoshita, M., ... Nishikawa, S. (2005). Characterization of mesendoderm: A diverging point of the definitive endoderm and mesoderm in embryonic stem cell differentiation culture. *Development*, 132, 4363–4374. <https://doi.org/10.1242/dev.02005>
- Teo, A. K., Arnold, S. J., Trotter, M. W., Brown, S., Ang, L. T., Chng, Z., ... Vallier, L. (2011). Pluripotency factors regulate definitive endoderm specification through eomesodermin. *Genes & Development*, 25, 238–250. <https://doi.org/10.1101/gad.607311>
- Tesar, P. J., Chenoweth, J. G., Brook, F. A., Davies, T. J., Evans, E. P., Mack, D. L., ... McKay, R. D. (2007). New cell lines from mouse epiblast share defining features with human embryonic stem cells. *Nature*, 448, 196–199. <https://doi.org/10.1038/nature05972>
- Van Den Aemele, J., Tiberi, L., Bondue, A., Paulissen, C., Herpoel, A., Iacovino, M., & Vanderhaeghen, P. (2012). Eomesodermin induces Mesp1 expression and cardiac differentiation from embryonic stem cells in the absence of Activin. *EMBO Reports*, 13, 355–362. <https://doi.org/10.1038/embor.2012.23>
- Viotti, M., Nowotschin, S., & Hadjantonakis, A. K. (2014). SOX17 links gut endoderm morphogenesis and germ layer segregation. *Nature Cell Biology*, 16, 1146–1156. <https://doi.org/10.1038/ncb3070>
- Zaret, K. (1999). Developmental competence of the gut endoderm: Genetic potentiation by GATA and HNF3/fork head proteins. *Developmental Biology*, 209, 1–10. <https://doi.org/10.1006/dbio.1999.9228>
- Zhao, R., Watt, A. J., Battle, M. A., Li, J., Bondow, B. J., & Duncan, S. A. (2008). Loss of both GATA4 and GATA6 blocks cardiac myocyte differentiation and results in acardia in mice. *Developmental Biology*, 317, 614–619. <https://doi.org/10.1016/j.ydbio.2008.03.013>

How to cite this article: Inamori S, Fujii M, Satake S, et al. Modeling early stages of endoderm development in epiblast stem cell aggregates with supply of extracellular matrices. *Develop Growth Differ*. 2020;62:243–259. <https://doi.org/10.1111/dgd.12663>